# FINAL REPORT FOR SUPRATHERMAL ELECTRONS IN A SOLAR ECLIPSE

CONTRACT NUMBER: NASw 2003

Dr. G.W. Sharp, Principal Investigator



Lockheed

MISSILES & SPACE COMPANY

A GROUP DIVISION OF LOCKHEED AIRCRAFT CORPORATION

SUNNYVALE, CALIFORNIA

# FINAL REPORT FOR SUPRATHERMAL ELECTRONS IN A SOLAR ECLIPSE

CONTRACT NUMBER: NASw 2003

Dr. G.W. Sharp, Principal Investigator

Prepared by

LOCKHEED PALO ALTO RESEARCH LABORATORIES

3251 Hanover Street

Palo Alto, California

for

NATIONAL AERONAUTICS AND SPACE ADMINISTRATION

Washington, D.C.

## SUMMARY

This final report describes the results of efforts to study the changes in the suprathermal electron flux caused by the total solar eclipse of March 7, 1970. The measurement was made with a retarding potential analyzer, mounted to view out the side of the rocket on Nike-Apache 14.457, which was launched from Wallops Island, Virginia at 1336:30 Local Time, March 7, 1970. For comparison a control experiment was conducted in which an identical analyzer was flown, mounted looking out the side of Nike-Apache 14.456, from Wallops Island at the same local time but on the previous day, March 6, 1970. Differential photoelectron flux in the energy range, 3 to 50 electron volts, and in the altitude range 120-180 km was measured both during the solar eclipse of March 7, 1970 and the day before at the same local time. The differential electron flux energy spectrum measured within totality had the same shape, but was a factor of ten smaller than that measured on the control day for altitudes between 120 and 180 km. This result directly implies that ionizing radiation responsible for the E and $F_1$ ionospheric regions was reduced by a factor of ten during totality. The differential flux spectra measured on the control day have the same general energy dependence as that reported by Doering et al. (1970) in the same altitude interval but the levels are larger by a factor varying from two to ten depending on altitude.

CONTENTS

LIST OF FIGURES

# SUPRATHERMAL ELECTRONS IN A SOLAR ECLIPSE

## INTRODUCTION

Energy from solar radiation is deposited in the upper atmosphere by photoionization of neutral gas particles. In this process an electron is released which usually has kinetic energy greatly in excess of the thermal energy of the ambient gas. This excess kinetic energy is given up eventually through collisons with thermal electrons, ions, and neutral gas particles. Theoretical work by Hanson and Cohen (1968) has shown that near the equator, on the average, the initial energy of the photoelectrons is 15 eV. At moderate-to high magnetic latitudes the fast photoelectrons created at altitudes above 300 km do not deposit their energy locally but are free to travel along field lines to the conjugate hemisphere (Hanson, 1963; Carlson, 1966).

The March 1970 Solar Eclipse, having a path of totality crossing Wallops Island, provided a unique opportunity to study the decay of the local suprathermal electrons which were created by prior photoionization and the energy distribution of photoelectrons streaming into the eclipse area from the solar illuminated conjugate hemisphere. A study of these electrons during the eclipse should lead to a more complete understanding of the energy balance of the upper atmosphere and the possible atmospheric processes taking place there.

One of the uncertainties in deriving recombination coefficients for the E and $F_1$ ionospheric layers from solar eclipse measurement arises from uncertainty in the eclipse function E(t). If at totality the local ionizing radiation is assumed equal to zero (E(t) = 0), the deduced recombination coefficient, $\alpha$, is of the order of $10^{-8}$ $cm^3$ $sec^{-1}$. It is of the order of $10^{-7}$

$cm^3$ $sec^{-1}$ if E(t) is assumed equal to about 0.1 at totality. Laboratory measurements of $\alpha$, measurements of residual 10.7 cm solar radio flux at totality, and rocket measurements of residual x-ray fluxes in the 44-60 Å range - part of the flux responsible for production of ionization in the E layer - suggest that E(t) should be of the order of 0.1 at totality (see Rishbeth, 1968 for review). We present herein measurements of the photoelectron differential flux distribution in the E and $F_1$ layers during totality of the 7 March 1970 eclipse and at the same local time the day before which indicate that E(t) = 0.1 at totality over the altitude range of 120-180 km.

Photoelectrons play an important role in the physics of the ionosphere and several computations of the photoelectron spectrum have been made (Hoegy et al., 1965; Nagy and Banks, 1970; Nisbet, 1968; Dalgarno et al., 1969). However, few measurements of the spectrum have been made - particularly in the lower ionosphere. The results of the present study are of significance for comparison with theory and other measurements in this lower altitude region.

## INSTRUMENTATION

Electron flux measurements were made with identical retarding potential analyzers (RPA) mounted on each of two Nike-Apache rockets, NASA 14.456 and NASA 14.457, which were launched from Wallops Island, Virginia at approximately 1836 UT on 6 March and 7 March 1970, respectively. Hereafter, results obtained on 6 March 1970 will be referred to as non-eclipse results. The RPAs were of the planar type with cylindrical cases (Figure 1). We define the RPA axis as the outward normal to the front surface of the instrument

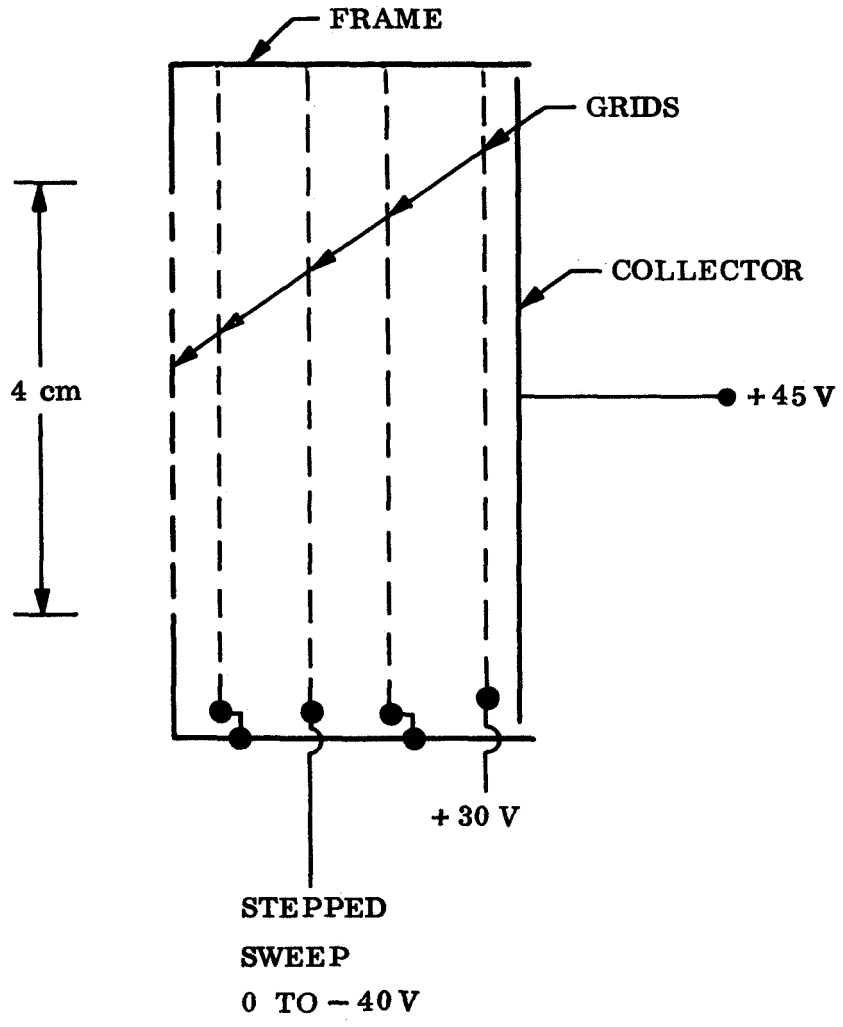


Figure 1 Schematic diagram of the retarding potential analyzer

coincident with the axis of the cylinder. The RPA axis was perpendicular to the rocket axis and looked, together with other sensors, through an elongated opening in the side of the rocket. The minimum half look angle of the RPA was $60^{\circ}$.

Figure 1 illustrates the RPA in approximately correct geometric proportion. Grids consisted of 100 mesh, 1 mil knitted tungsten screen, and these and all other conducting surfaces were gold plated. The first, second, and fourth grids were grounded, and the fifth was maintained at +30V to suppress secondary electron emission from the collector which was maintained at +45 volts. The positive potential on the collector prevented the collection of ambient positive ions. The retarding grid voltage was cycled through a series of constant values with each value held constant for a period exceeding the spin period of the rocket. The retarding grid voltages included integer values from 0 to -10 volts and multiples of 5 from 0 to -40 volts. The electrometer had a logarithmic response to electron current and was calibrated periodically throughout the flight by disconnecting it from the collector and alternately connecting it to a large ($10^{-7}$ amp) and small ($10^{-10}$ amp) constant current source.

## DATA REDUCTION

A sample of the telemetry signal from the non-eclipse rocket is illustrated in Figure 2. The periodic current pulses occurred as the RPA axis rotated into the sun. When the RPA rotated through the shadow cast by the rocket, the current was essentially constant with some exception to be noted. The electrometer current is not saturated during direct solar illumination. Failure of a change in retarding potential to noticeably change

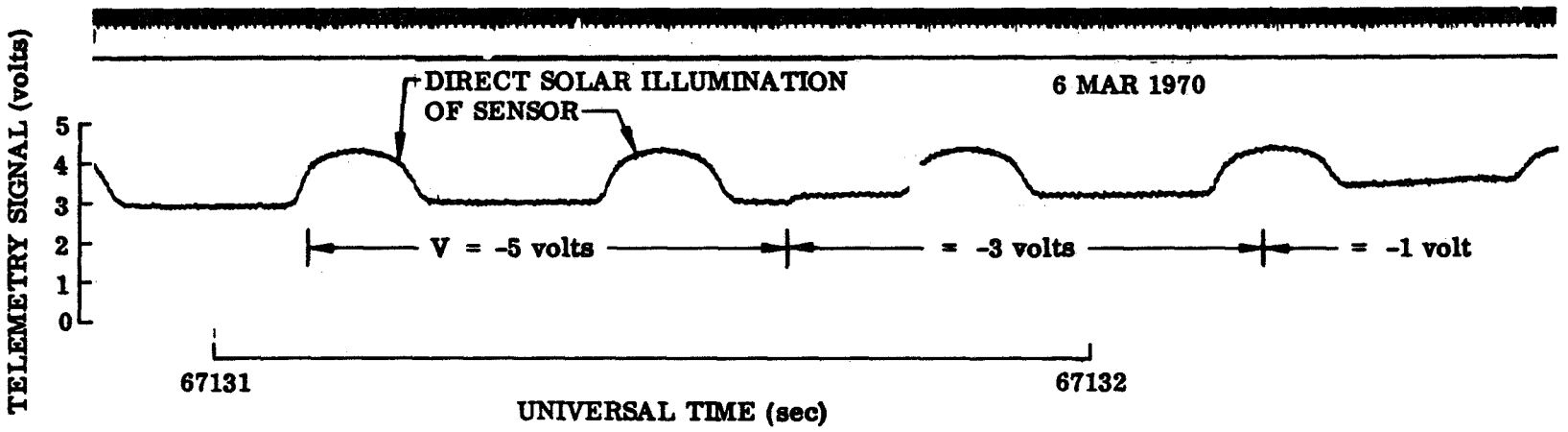


Figure 2 Sample of the electrometer telemetry signal from non-eclipse flight

the current during direct solar illumination is an indication that the current is largely photoelectron current emanating from surfaces at or behind the retarding grid of the RPA. A change in ambient photoelectron current is evident when V, the retarding potential, changed from -5 to -3 volts with the RPA in the solar shadow of the rocket.

The telemetry signals for both rockets were digitized and converted to appropriate voltages and collector current, the latter being done consistent with laboratory and inflight calibration of the electrometer sensitivity. The results were displayed by computer, a sample of which is shown in Figure 3 for the eclipse rocket. The sensor current was not plotted within a small time interval centered on the instant of retarding potential change. Although the rocket is in eclipse, a current pulse resulting from direct solar exposure of the RPA is again evident. The solar current pulse is comparable in magnitude to the shadow current during non eclipse (see Figure 11). The current is observed to be essentially constant while the RPA rotates through the solar shadow with the exceptions of the 0 and -1 volt steps. At these retarding voltages the current was typically 10 to 20% lower just after rotating out of the sun. This latter behavior may result from photoelectrons emanating from the rocket surfaces - a possibility discussed in more detail in Appendix II.

RPAs measure an integral of the differential electron flux with energy above a threshold determined by the retarding potential. To obtain the mean differential flux, the difference in integral flux for two retarding potentials is divided by an effective energy integral defined by the two retarding potentials.

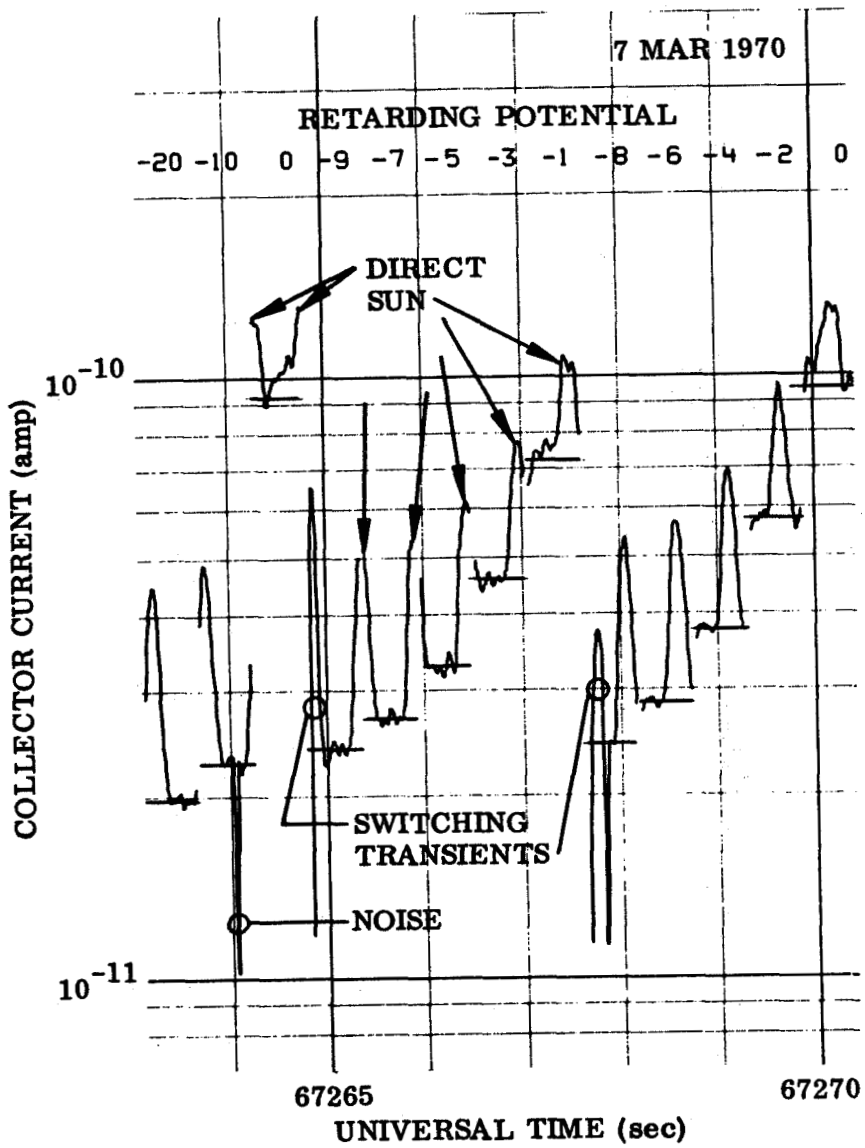


Figure 3 Computer drawing of reduced electrometer signal from eclipse flight

Two possible energy integrals are illustrated in Figure 4 for the retarding potentials -2 and -4 volts. The area under the solid transmission curve is the energy integral appropriate to the present instrumentation for an assumed isotropic electron flux in the undisturbed plasma. The cross hatched area within the dashed transmission curve is the energy integral appropriate to an electron flux entirely parallel to the RPA axis.

The energy assigned to the mean flux for the -2, -4 volt interval is that labeled $E_{k_j}$ in Figure 4 and is the energy at which the mean flux, derived in the above manner with use of the solid curve, would equal the actual flux for an assumed power law dependence of differential electron flux on energy. The energy labeled $E^*_{k_j}$ is the corresponding energy derived with the use of the cross hatched energy integral. We have found that the energy integral used in deriving the mean differential flux is nearly the same for both the solid and dashed transmission curves. However, the energy to be assigned the mean flux is significantly different for the two curves. The use of $E^*_{k_j}$ instead of $E_{k_j}$ would lower the derived flux by approximately a factor of three for the power law spectrum fitting the data. The flux values presented herein were derived using transmission curves appropriate to an isotropic electron distribution such as that illustrated by the solid line of Figure 4. A more detained description is given in Appendix I.

The resolution of the RPAs, $E/\Delta E$, is not large-about two for most of the data if $\Delta E$ is defined as the half width of the transmission curve and E is the value of $E_{k_j}$.

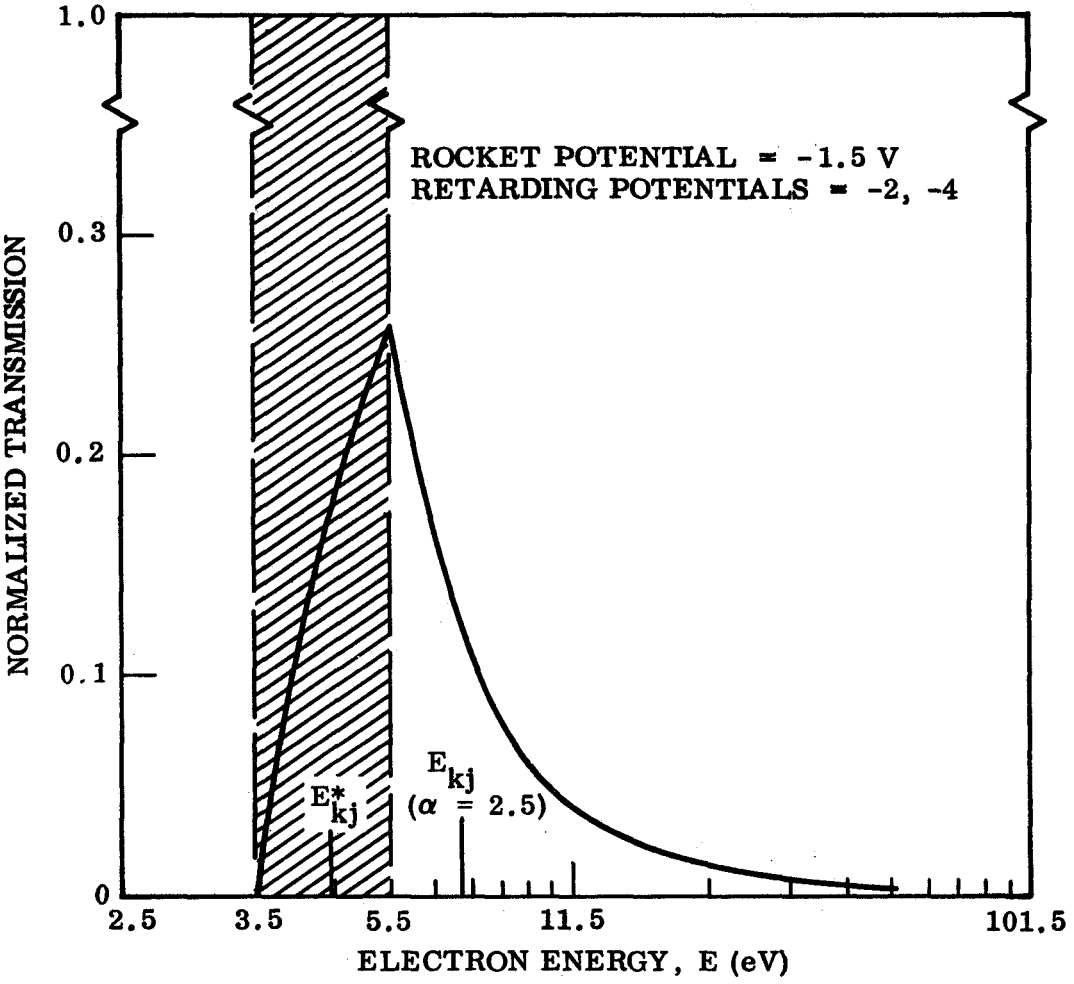


Figure 4 Typical energy transmission curve and corresponding energy assignment for a flux distribution normal to the RPA axis (dashed) and isotropic (solid) within the undisturbed plasma

Measurements of low energy electron flux are subject to error from electron shadowing and non-ambient photoelectron contamination. Electron shadowing occurs when the vehicle intercepts electrons spiralling in the magnetic field of the earth which would have entered the instrument had the vehicle not been present. Non-ambient photoelectron contamination refers to electron current collected by the RPA which arises from photoelectrons emanating from solar exposed surfaces of the vehicle. The RPAs were not mounted optimally for suppression of these two types of errors in the present experiment. We have concluded from an analysis of the results that neither of these two types of error is likely to be serious. The analysis is detailed in Appendix II.

The vehicle potential, $\varphi$, was not measured by instrumentation included in the payloads and has been assumed equal to -1.5 volts for each flight. The actual value is likely to have been between -1 and -2 volts. Uncertainty in $\varphi$ introduces uncertainty in the value of $E_{k_j}$ not only through the change in abscissa values but also in the shape of the transmission curve in Figure 4. The error is discussed more fully in Appendix I.

## RESULTS

### Non-Eclipse Electron Flux

The non-eclipse differential flux is illustrated in Figure 5 for a number of heights. The error bars at low energy result from uncertainty in the vehicle potential as explained previously. The estimated uncertainty at the high-energy portion of the curves is that resulting from subtracting two signals containing some noise which are nearly equal in magnitude. The

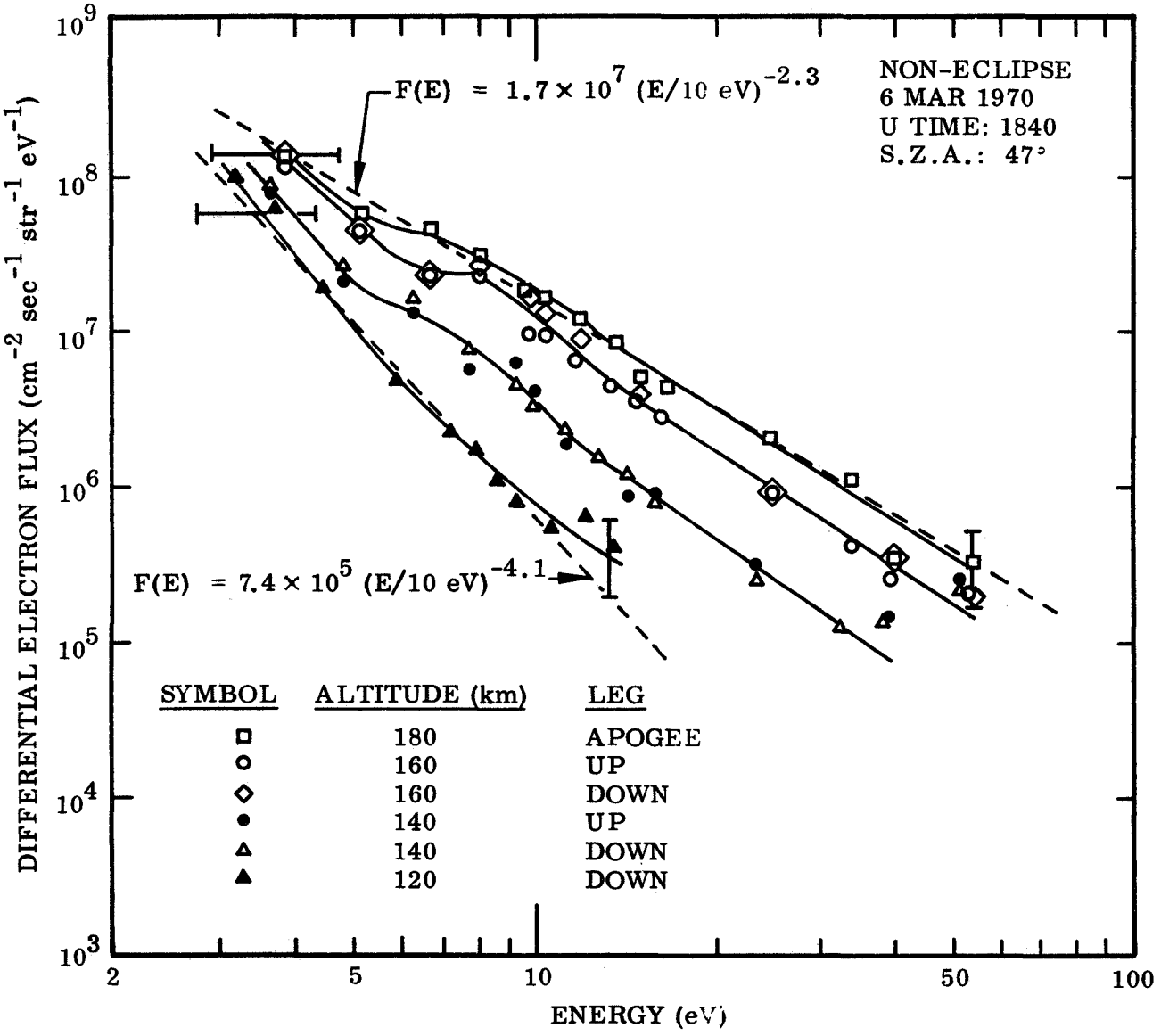


Figure 5 Differential flux observed during the non-eclipse flight. The measured spectra vary approximately with energy according to a power law dependence, two of which are illustrated by the dashed lines, together with the corresponding analytic expression. The units of F(E) and E in the analytic expressions are those appropriate to the ordinate and abscissa of the figure respectively

spectrum was observed to be the same on both the up and down legs within the experimental uncertainty. Antennae for another experiment were still being deployed at 120 km on the up leg and consequent noise prevented a reliable spectrum to be derived at that altitude. A small amount of structure appears to be present, and the solid lines represent our interpretation of the smoothed spectra. To a good approximation, the spectra may be represented by a simple power law dependence on energy. Two are indicated by the dashed lines together with their analytic expression. The units of F and E are those of the ordinate and abscissa respectively.

Figure 6 compares the present results with rocket results of Doering et al. (1970) obtained under rather similar conditions. The results of Doering et al., were obtained with much higher instrumental resolution and with the sensor in a more ideal location to reduce electron shadowing and non-ambient photoelectron contamination. The results at Doering et al. at 120 and 180 km were obtained on the down leg of their rocket flight and are a factor of two larger than those obtained on the up leg. We include their results at 290 km for comparison with the present results at energies between 25 and 50 eV.

We consider the results at 180 km altitude obtained in the two experiments to be in good agreement with exception of the difference in shape between approximately 5 and 15 eV. The present results are convex while those of Doering et al. are concave in this energy interval. It is believed this difference can not be attributed to differences in instrument resolution. An immediate suspected cause is non-ambient photoelectron contamination. However, we would expect any such contamination to be most severe at around 4 eV energy because of the large Lyman-$\alpha$ photon flux. We

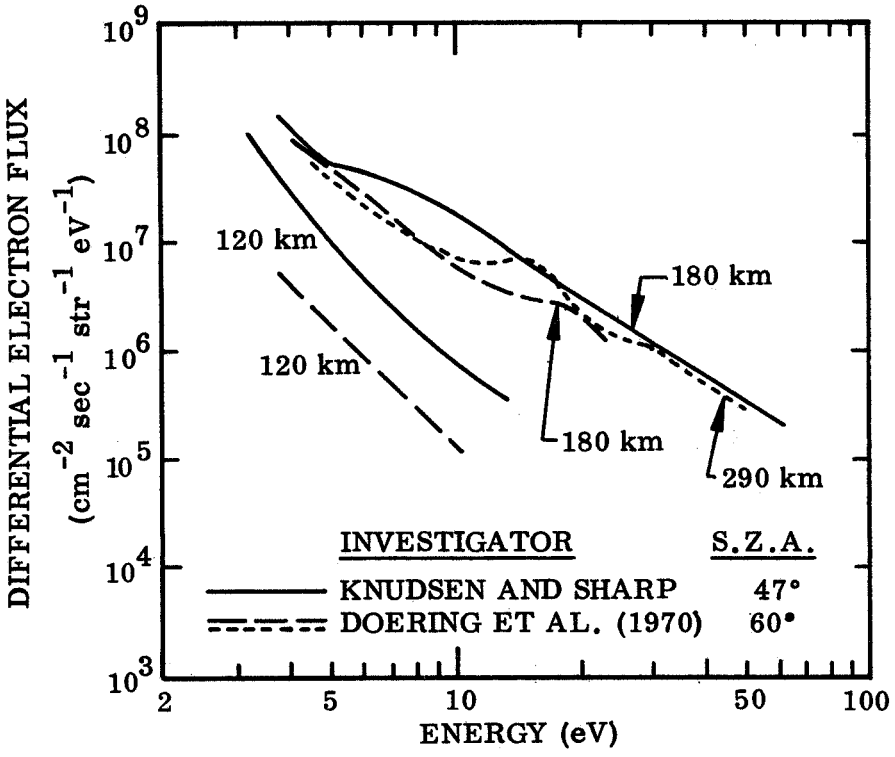


Figure 6 Comparison of the present results with experimental results recently reported by Doering et al. (1970)

shall see that the photoelectron spectrum did not change in shape during the eclipse even though the Lyman-$\alpha$ photon flux was reduced much more during the eclipse than was the more energetic photon flux responsible for E and $F_1$ layer ionization (Smith, 1971; Accardo et al. 1971).

The apparent factor-of-two difference in magnitude may not be real. Doering et al. have indicated an uncertainty of 1.5 in their instrumental geometric factor, and the uncertainty in the present flux levels resulting from vehicle potential uncertainty is at least a factor of 2. However, if the difference is real, it is in the direction to be expected. The extreme ultraviolet solar intensity as inferred from the 10.7 radio flux was larger and the solar zenith angle smaller for the present results than those of Doering et al. Both conditions would make the present photoelectron flux the larger of the two.

The two sets of results are in less satisfactory agreement at 120 km. The energy dependence is essentially the same for both results, but the present results are a factor of 5 larger in magnitude even after adjusting the two sets to agree at 180 km. This discrepancy in magnitude is not understood.

In Figure 7 the present results are compared with theoretical predictions by Dalgarno et al. (1969) and Nagy and Banks (1970). Not as much structure appears in the experimental results as predicted by Dalgarno et al. We had insufficient resolution to see the structure predicted by Nagy and Banks. The most serious discrepancy between our experimental results and these predictions is in the level of flux expected at 120 km. The experimental results are larger than expected.

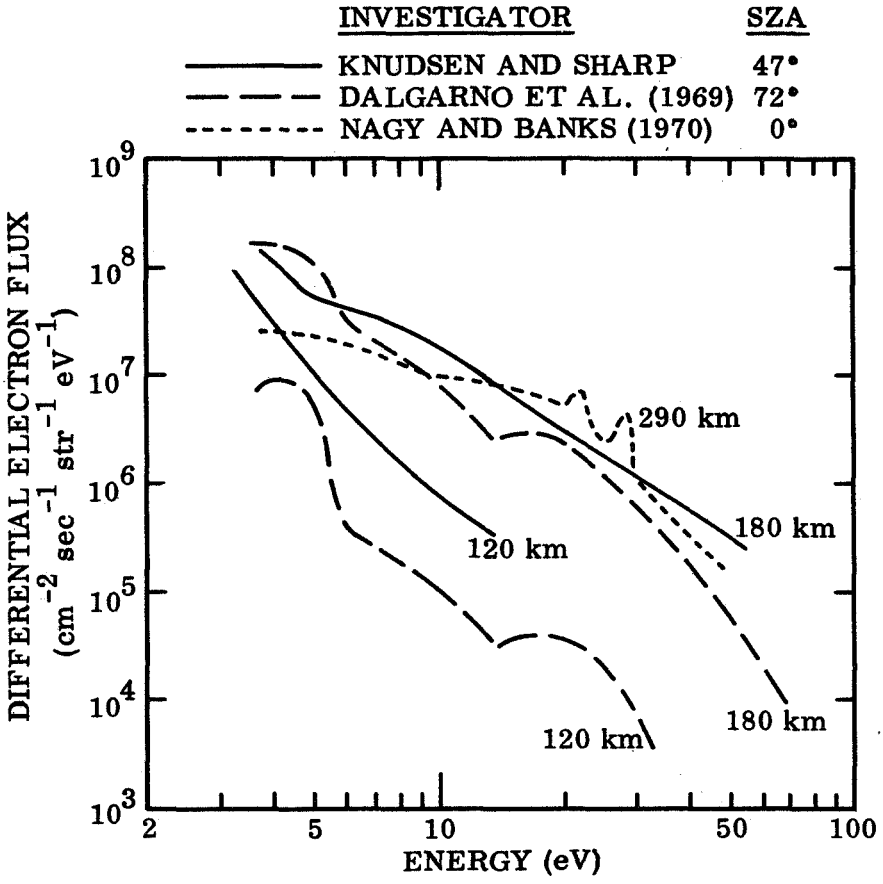


Figure 7 Comparison of the present results with theoretical spectra calculated by Dalgarno et al. (1969) and Nagy and Banks (1970)

Eclipse Electron Flux

The measured eclipse and non-eclipse electron flux at 180 km altitude are compared in Figure 8. Similar results for 120 km altitude are illustrated in Figure 9. At both altitudes the shapes of the spectra remained unchanged in eclipse within experimental accuracy. The flux levels were reduced a factor of 10 ± 1 at both altitudes.

An immediate conclusion to be drawn from the results in Figures 8 and 9 is that the cumulative EUV and x-ray photon flux responsible for producing the ionization between 120 and 180 km was reduced by the same factor, namely, 10. Since the photoelectrons have a lifetime short compared with the eclipse time, the photoelectron flux will be in a continuous steady state. We may write an energy balance equation

$$P(E) = f(E)\, L(E)$$

where P(E) is the production rate of photoelectrons per unit volume with energy between E and E+dE from direct photoelectron processes as well as cascade processes, f(e) is the photoelectron concentration within the same energy interval, and L(E) is the loss rate out of the energy interval. The loss rate L(E) depends only on atomic processes and the neutral atmospheric composition and concentration. At the altitudes of interest, loss from elastic collisions with electrons is a minor loss process. Also, transport is negligible. Hence, the photoelectron concentration, f(E), and, consequently, flux, F(E), will change in direct proportion to P(E) during the eclipse provided the neutral atmosphere does not change. The experimental evidence that F(E) was reduced a factor of 10 during the eclipse directly implies that P(E) was reduced by the same factor for E between 3 and 50 eV.

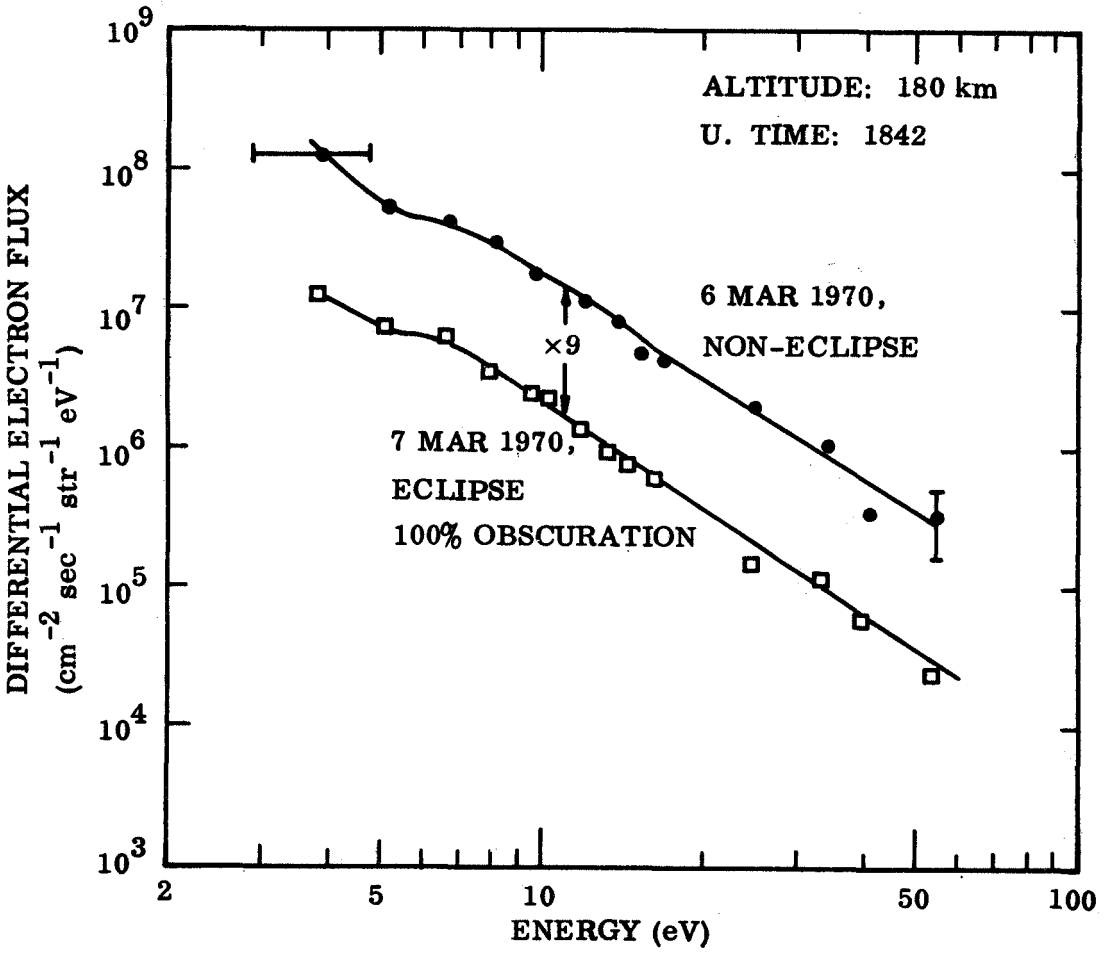


Figure 8 Comparison of eclipse and non-eclipse differential electron flux spectra at 180 km altitude.

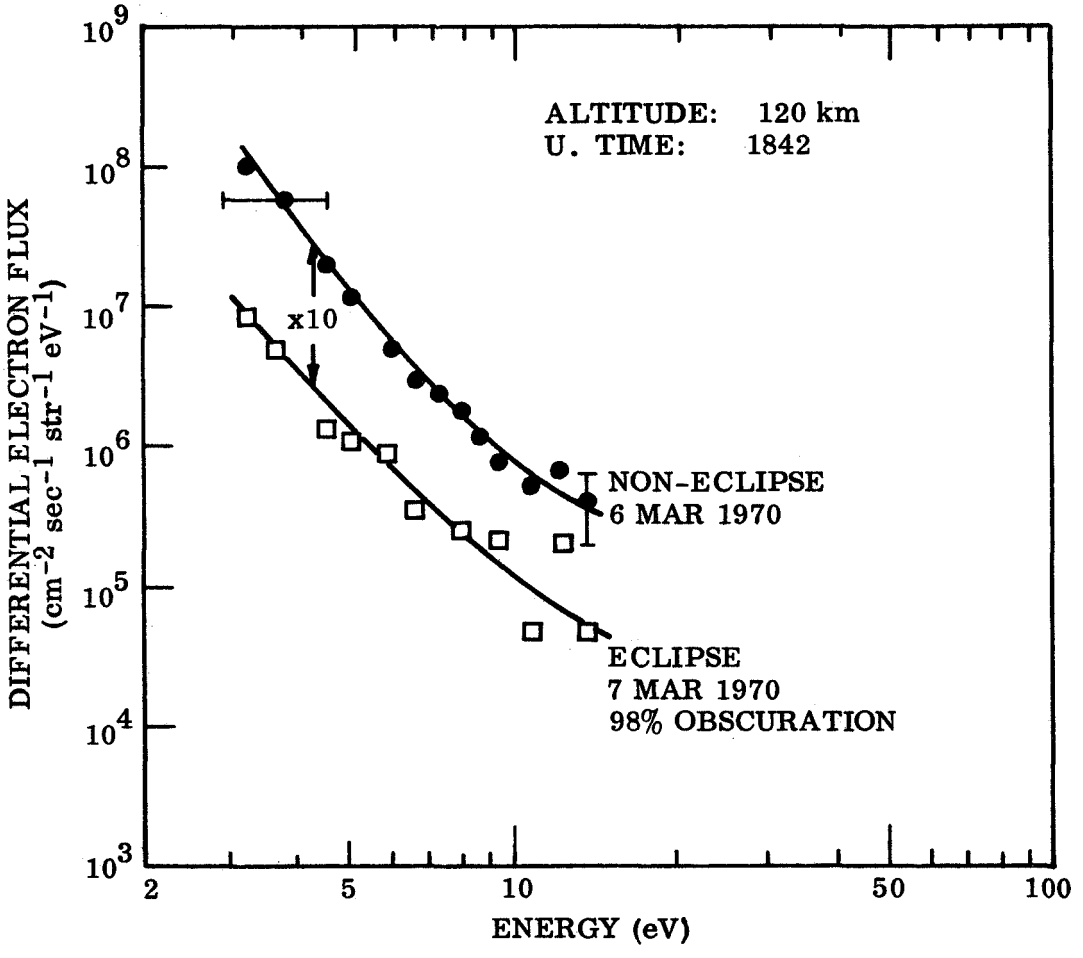


Figure 9 Comparison of eclipse and non-eclipse differential electron spectra at 120 km altitude

The above results -- to the extent they represent the ambient photoelectron flux and not photoelectron fluxes from the rocket surfaces -- independently support the conclusion that the eclipse function E(t) is reduced to only 0.1 during totality in both the E and $F_1$ layers. It has been recognized previously as outlined in the introduction, that E(t) should have a minimum value of ~ 0.1 if eclipse deduced recombination coefficients are to approach laboratory measured values. Other direct evidence that the eclipse function was reduced a factor of ten in the E region during the 7 March 1970 eclipse has been presented by Accardo et al. (1971). They observed that x-rays in the wavelength range 44-60 Å, which are a portion of the spectrum responsible for the E region ionization, were reduced to 16 percent of the full sun value during totality.

Conjugate Photoelectron Flux

Maier and Rao (1971) have reported measurement of photoelectron flux during totality of the 7 March 1970 eclipse. Their measurement was made with an RPA mounted on the nose of a rocket with instrument axis parallel to the rocket spin axis and essentially parallel to the magnetic field. Further, the spin axis of the rocket was oriented such that the face of the RPA was not exposed to direct solar illumination (private communication). Consequently, their results should contain no non-ambient photoelectrons emitted from the rocket surface, and no vehicle shadowing should exist. In Figure 10 their spectrum, representative of their results from 215 to 263 km altitude, is presented together with our results at 180 km. Maier and Rao's results have been divided by $\pi$ to compare directly with our results. That is, the flux per unit solid angle is obtained from the flux

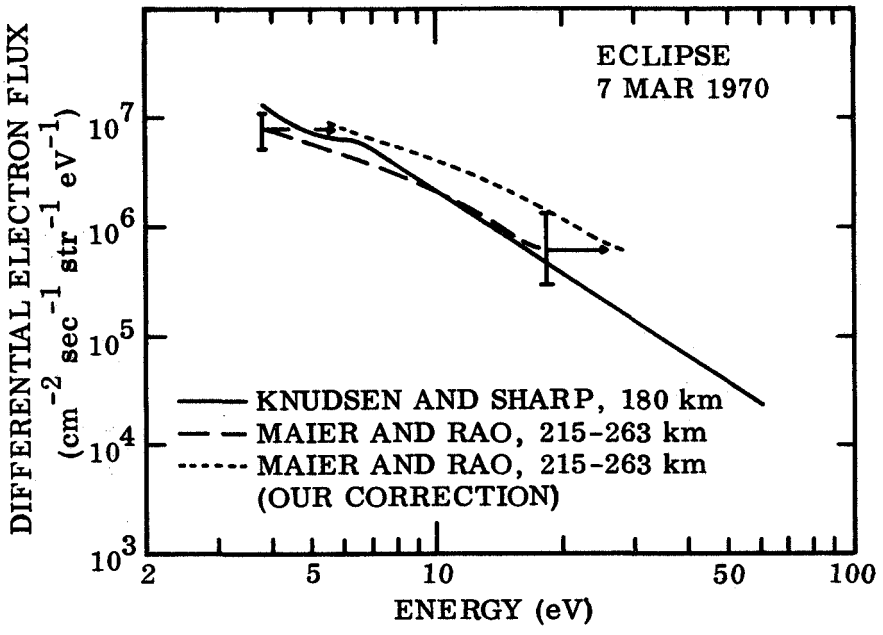


Figure 10 Comparison of the present differential electron flux with that reported by Maier and Rao (1971) both of which were measured within totality

impinging on a plane surface by division by $\pi$ provided the flux is isotropic as we are assuming. The dotted curve is our estimate of their results had energy been assigned to their mean flux values in the same manner as was used for our results. With similar data reduction, the present results are somewhat lower than those of Maier and Rao as expected from theoretical predictions (Dalgarno et al., 1969).

Maier and Rao have interpreted their observed flux to be a flux of electrons from the undisturbed conjugate ionosphere. The rather good agreement in magnitude in the two observations suggests that a significant local contribution to their measured electron flux may have existed. The fluxes observed by us are sufficiently low in the atmosphere that they should be locally produced. Nagy and Banks (1970) have calculated the attenuation of low energy electron fluxes (5 to 100 eV) impinging upon the atmosphere from above ($T_\infty$ = 1000°K) and found reductions of several orders of magnitude at an altitude of 200 km. Consequently, a locally produced electron flux similar in magnitude to that observed by us should have existed in the altitude range of Maier and Rao's results.

Another point of interest in the results of Maier and Rao (1971) is a small enhancement of flux at approximately 7-9 volts. The summary of results between 215 and 263 km altitude reproduced in Figure 10 does not show the enhancement, but three of four individual spectra presented by them do show an enhancement. Our results (Figure 5) show a small but significant enhancement centered at approximately the same energy.

## CONCLUSIONS AND RECOMMENDATIONS

The present study of the 1970 Solar Eclipse at Wallops Island has shown that the ionizing radiation responsible for the E and $F_1$ ionosphere is reduced by a factor of ten during totality. It is not necessary that all eclipses would have the same reduction factor. Thus a measurement like the one described herein would be appropriate to perform during future eclipses, especially for the 1973 eclipse in Western Africa. A control experiment performed in connection with that particular eclipse would be of great value since it will be during solar minimum conditions and performed at low latitudes where the small inclination of the earth's magnetic field will substantially reduce possible photoelectron flux contamination which clouds the March 1970 results to some extent.

To perform a study of the conjugate effects during an eclipse would require flying instrumentation to heights well above 300 km in middle to upper latitudes. The present study did not go to high enough altitude to be effect for this. This would be a really valuable measurement to make during an eclipse. However, the 1973 eclipse is occurring at latitudes that are too low to provide the information needed for this study. Future eclipses should be examined for the possibility of being able to make this important measurement.

## NEW TECHNOLOGY

No new technology has been developed from work under this contract.

# APPENDIX I

Retarding potential analyzers measure some integral of the electron flux having energy above some threshold energy. The method used in deriving a differential spectrum from the measured currents is presented below.

The electron current, I, to the collector of the RPA may be written as

$$(1) \qquad I(V, \varphi) = 2\pi e \int_{E' = 0}^{\infty} \int_{r = 0}^{R} \int_{\theta = 0}^{\frac{\pi}{2}} F'(E', \theta, \varphi) T'(E', \theta, r, V) \cdot \sin\theta \cos\theta \, 2\pi r \, dr \, d\theta \, dE'$$

where e is the charge on the electron (negative), $E'$ is the kinetic energy of the electron at the plane of the RPA front surface, r is the radial distance measured from the RPA axis, R is the radius of the RPA opening, $\theta$ is the polar angle measured from the inward normal to the RPA surface, $F'$ is the differential photoelectron flux in the plane of the RPA front surface (dimensions of area$^{-1}$ time$^{-1}$ energy$^{-1}$ solid angle$^{-1}$), V is the retarding potential relative to the RPA ground, $\varphi$ is the vehicle potential relative to the undisturbed plasma, and $T'$ is the transmission function of the RPA. We have assumed that the plasma sheath is sufficiently thin that it may be considered plane and that the differential flux is not azimuth dependent. If the differential flux within the undisturbed plasma, F(E) is assumed isotropic, it will become anisotropic is passing through the plane sheath and be related to $F'$ by the formula

$$(2) \qquad F'(\theta, E', \varphi) = \frac{(1 - E_o/E)}{(1 + \frac{E_o}{E} \mathrm{Tan}^2\theta)^{1/2}} \; F(E),$$

a result derivable from application of Liouville's theorem, where

$$E = Eo + E'$$

and

$$Eo = e\varphi$$

Inserting equation 2 into 1, we obtain

$$(3) \qquad I(V, \varphi) = \pi R^2 e \int_0^\infty F(E)T(E, V, \varphi)dE$$

where

$$(4) \quad T(E, V, \varphi) = \frac{2}{\pi R^2} \frac{E - Eo}{E} \int_{r=0}^{R} \int_{\theta=0}^{\frac{\pi}{2}} \frac{T'(E, \theta, r,, V)}{(1 + \frac{Eo}{E} \operatorname{Tan}^2\theta)^{1/2}}$$

$$\cdot \sin\theta \cos\theta \, d\theta \, 2\pi r dr; \; E \geq Eo$$

$$= 0 \; ; E \leq Eo.$$

T is a normalized transmission function which would be 1 for $E > Eo$ for an idealized instrument that counted all electrons entering the aperature.

The cumulative current, $I_k$, measured with retarding potential equal to $V_k$ becomes

$$(5) \qquad I_k = \int_0^\infty F(E)T_k dE$$

where we have used the short hand notation

$$T_k = T(E, V_k, \varphi).$$

A mean differential flux $\overline{F_{kj}}$ may be defined as

$$(6) \qquad \overline{F_{kj}} = \frac{\int_0^{E_m} F(E) t_{kj} dE}{\int_0^{E_m} t_{kj} dE}$$

where

$$(7) \qquad t_{kj} = T_k - T_j$$

and $E_m$ is some sufficiently large energy. Now, $t_{kj}$ approaches zero for E much larger than the larger of $eV_k$ and $eV_j$, a fact known from numerical integration of T as will be presently shown and F(E) varies approximately as

$$(8) \qquad F(E) = F_{Eo} \left(\frac{E}{Eo}\right)^{-\alpha}$$

with $\alpha$ at least as large as 2.

Hence, we have

$$(9) \qquad \overline{F_{kj}} = \frac{I_k - I_j}{\int_0^{E_m} t_{kj} dE} - \frac{\int_{E_m}^{\infty} F(E) t_{kj} dE}{\int_0^{E_m} t_{kj} dE}$$

By taking $E_m$ sufficiently large, the last term on the right of equation 9 may be made smaller than the experimental uncertainty in the $I_k$ and

$$(10) \qquad \overline{F_{kj}} = \frac{I_k - I_j}{\int_0^{E_m} t_{kj} dE}$$

The transmission functions, $t_{kj}$, have been evaluated for the RPA used in this experiment by numerically performing the integration indicated in euqation 4 for all voltage steps $V_k$ applied to the retarding grid and for assumed values of $\varphi$ equal to -1, -1.5 and -2 volts respectively. Electron flux trajectories were followed from the entrance grid to the collector with the flux reduced by the appropriate angle dependent transmission at each grid. Fluxes with trajectory encountering the walls of the cylindrical frame were set to zero. The trajectories were determined by the initial trajectory at the entrance and the electric fields between grids and grid and collector. The potential in the plane of each grid was assumed constant.

A plot of $t_{kj}/T'(\infty, 0, 0, V)$ for $V_k$, $V_j$ and $\varphi$ equal to -2, -4, and -1.5 volts respectively is shown in Figure 4. Had the finite radius of the RPA walls and collector, the angular dependence of the grid transmission, the effect of $\varphi$ on the differential flux, and the influence of the electric fields between grids on electron trajectory been neglected in computing $t_{kj}$, the dashed line behaviour would have been obtained. The dashed line behaviour is that generally assumed in reducing RPA data.

We have found that the integral

$$(11) \qquad \mathcal{L}_{kj}(E_m) = \int_o^{E_m} t_{kj}\,dE$$

when integrated to 500 eV is only 10 to 20% less than would have been derived from thatassuming the simplified behaviour such as that indicated by the dashed line in Figure 4. The correction to the $F_{kj}$ from use of the more accurate $t_{kj}$ would appear to be insignificant. What is significant, however, is the change in the energy, $E_{kj}$, to be associated with the values of $\overline{F_{kj}}$.

Since F(E) is the actual differential flux behaviour, we desire a value of $E_{kj}$ such that

$$(12) \qquad \overline{F_{kj}} = F(E_{kj}).$$

If we assume for the present that F(E) is of the form

$$(13) \qquad F(E) = F(Eo)(E/Eo)^{-\alpha},$$

then

$$(14) \qquad E_{kj} = Eo(F_{kj}/F(Eo))^{-1/\alpha}$$

$$= \left( \frac{\int_{E_o}^{E_m} E^{-\alpha} t_{kj}\,dE}{\int_{E_o}^{E_m} t_{kj}\,dE} \right)^{-1/\alpha}$$

Equation 14 makes clear that the shape of $t_{kj}$ is important in determining $E_{kj}$. In Table 1 we list a number of values of $\mathcal{L}_{kj}(E_m)$ and $E_{kj}$ for an $E_m$ of 500 eV and $\alpha$ of -2.5 and -4.0. $\mathcal{L}^*_{kj}$ is the integral corresponding to equation 11 where $t_{kj}$ is the simplified behavior given by the dashed line in Figure 4, and $E^*_{kj}$ is the corresponding energy given by equation 14. $E^*_{kj}$ did not change significantly with $\alpha$ in the range indicated. Consideration of cases 1, 2, and 3 of Table I indicates that use of $\mathcal{L}^*_{kj}$ instead of $\mathcal{L}_{kj}$ in deriving $\overline{F_{kj}}$ would lower these values at most by 25%, but the use of $E^*_{kj}$ rather than $E_{kj}$ for the case of $\alpha = 2.5$ would shift the plot of $F_{kj}$ vs $E_{kj}$ to the left an amount equivalent to reducing the $F_{kj}$ by factors of approximately 5 and 2.5 at energies of 2 and 30 eV respectively. Cases 4 and 5 illustrate that the values of $E_{kj}$ change more than the change in $E_o$ which is proportional to the change in $\varphi$. Similar cases not shown were used to derive the estimated error from the uncertainty in $\varphi$. Values of $E_{kj}$ and $E^*_{kj}$ corresponding to the solid and dashed transmission functions are illustrated in Figure 4.

TABLE 1 DEPENDENCE OF $E_{kj}$ ON ASSUMED TRANSMISSION FUNCTION AND VEHICLE POTENTIAL

| Case | $\varphi$ Volt | $V_k$ Volt | $V_j$ Volt | $I_{kj}$ eV | $I^*_{kj}$ eV | $E_{kj}$ ($\alpha = 2.5$) eV | $E_{kj}$ ($\alpha = 4$) eV | $E^*_{kj}$ ($2.5 \leq \alpha \leq 4$) eV |
|---|---|---|---|---|---|---|---|---|
| 1 | -1.5 | 0 | - 1 | 0.75 | 1.0 | 3.8 | 3.2 | 1.9 |
| 2 | -1.5 | - 4 | - 5 | 0.90 | 1.0 | 9.6 | 8.6 | 6.0 |
| 3 | -1.5 | -20 | -30 | 7.5 | 10.0 | 39.5 | 36.2 | 26 |
| 4 | -1.0 | 0 | - 1 | 0.84 | 1.0 | 2.8 | 2.3 | 1.4 |
| 5 | -2.0 | 0 | - 1 | 0.69 | 1.0 | 4.8 | 4.0 | 2.5 |

## APPENDIX II

The mounting of the RPAs in the rockets was less than optimum and makes the results more subject to question than would have been the case with a more optimum mounting such as that recently used by Doering et al. (1970). We attempt below to evaluate the amount of electron shadowing and non-ambient photoelectron contamination that may exist in the results. To evaluate the amount of non-ambient photoelectron contamination that may have been present, it would be desirable to numerically compute the photoelectron differential flux - both the magnitude and angular distribution - that emanates from the solar exposed portions of the rocket and reaches the RPA. Such a task has not been attempted, but experimental evidence will be presented which suggests that contamination was not significant.

The amount of shadowing of the ambient photoelectron flux is believed to be less than 50%. The RPA was mounted near the forward end of the rocket with its axis normal to the spin axis of the rocket. With the spin aixs of the rocket parallel to the magnetic field, which is the worst possible case, down-going ambient photoelectron flux with pitch angle less than about seventy degrees and energy greater than 3 eV would not be shadowed. For the more energetic flux, pitch angles still closer to $90^{\circ}$ would be collected. Up-going photoelectron flux would essentially be cut off by the rocket.

In flight, the angle between the magnetic field and spin axis of the rocket varied as a result of rocket precession from $10^{\circ}$ to $21^{\circ}$ for the eclipse rocket and from $1^{\circ}$ to $25^{\circ}$ for the non-eclipse rocket. Plots of

the collector current at constant retarding potential as a function of time evidenced modulations correlated with the variation of this angle. The smallest current occurred when the angle was smallest - a result expected for electron shadowing. The maximum to minimum current variation was approximately 10% for the eclipse rocket (NASA 14.457) and 20% for the non-eclipse rocket (NASA 14.456).

The above considerations lead us to believe that the electron fluxes are at least 50% of what they would have been in the absence of any vehicle shadowing.

The constancy of the current as the RPA rotates through the solar shadow cast by the rocket suggests that no significant contamination from vehicle photoelectrons exists in these shadow intervals. Doering et al. (1970) reported observing vehicle photoelectrons when their instrument, which was extended from the rocket, was pointed toward the sun and away from the sun but not when pointed approximately at right angles to the sun. No similarly large enhancement is evidenced in Figure 3. Some indication of a small (5-10%) increase occurred on occasion such as the -6 and -4 volt steps (67268 sec interval). However, this small increase was not always anti-coincident with the sun pulse and is more likely the result of the change in electron shadowing as the angle between the instrument normal and the magnetic field varied at twice the spin period.

At retarding potentials of 0 and -1 volt, a small systematic increase in current (10-20%) did occur within the solar shadow interval as evidenced in Figure 3. The current was least as the rocket rotated clockwise (looking along the rocket velocity vector) into the rocket shadow and greatest as it rotated out of the shadow. Photoelectrons from the vehicle spiral counter clockwise (looking in the same direction) in the magnetic field of

the earth, and lower energy electrons from the vehicle surface could reach the RPA at the location it rotated out of the shadow than at the location of entry into the shadow. The solid angle at the source subtended by the RPA would be larger at exit than at entry, also. This qualitative evidence suggests that a small amount of contamination was occurring at the lowest two or three energy steps.

Another piece of evidence that non-ambient photoelectron contamination is negligible is presented in Figure 11. These two sets of curves, ECLIPSE and NON-ECLIPSE, of collector current vs retarding potential were recorded at nearly the same altitude and with the angle, $\gamma$, between rocket axis and sun vector equal. The curve labeled direct was derived by subtracting the current when the RPA was in the rocket shadow from the maximum current when it was looking most directly at the sun. Both currents were measured with constant retarding potential. If we assume for the present that the shadow current represents an ambient photoelectron flux, then the direct current as defined represents photoelectrons produced solely within the instrument and/or on the rocket surfaces. The reduction of this direct current by a factor of about 45 during the eclipse is a direct indication of the reduction of photoelectron production from the exposed surfaces of the rocket. Although the rocket surface is aluminum - its work function is a little less than that of gold - about the same distribution of photoelectrons as that from gold may be expected. The curves labeled SHADOW are the cumulative currents observed with the RPA looking away from the sun. If these currents consisted primarily of photoelectrons from the rocket, the reduction during eclipse should be similar to that of the direct current. The reduction was observed to be only about a factor of 5.

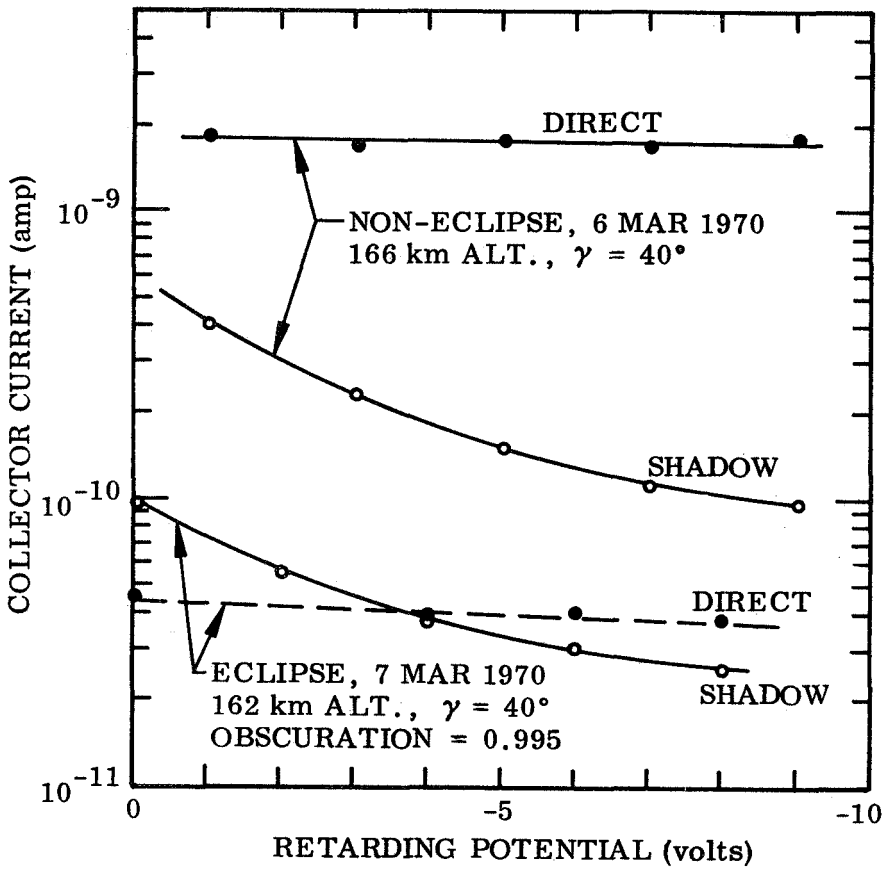


Figure 11 Collector current variation with retarding potential when the RPA was looking most directly at the sun (DIRECT) and when looking into the shadow cast by the rocket (SHADOW) for both the eclipse and non-eclipse flights. The angle $\gamma$ is that between the RPA axis and the rocket-to-sun vector at time the DIRECT collector current was measured.

Finally, and most convincing perhaps, the close agreement between the results of Maier and Rao (1971) and the present results suggests to us that non-ambient electron flux contamination was not serious in the present results -- at least not at 180 km altitude. As outlined previously, the results of Maier and Rao should be free of non-ambient photoelectron contamination, and if their measured flux is substantially locally produced as we have suggested, we would expect the flux as measured by us at 180 km to be somewhat smaller as is the case.

We conclude that significant non-ambient photoelectron contamination does not appear to be present but that the measured fluxes may be as small as 50% of what they would have been in the absence of electron shadowing.

REFERENCES


Accardo, C.A., L.G. Smith and G. Pintal, "Rocket observations of solar x-rays during the eclipse of 7 March 1970," paper A6.6, COSPAR, Fourteenth Plenary Meeting, Seattle, Washington, June 1971.

Carlson, H.C., Jr., "Ionospheric heating by magnetic conjugate-point photoelectrons." J. Geophys. Res., 71, 195, 1966.

Dalgarno, A., M.B. McElroy and A.I. Steward, "Electron impact excitation of the dayglow," J. Atmos. Sci., 26, 753, 1969.

Doering, J.P., W.C. Fastie and P.D. Feldman, "Photoelectron excitation of $N_2$ in the day airglow," J. Geophys. Res., 75, 4787, 1970.

Hanson, W.B., "Electron temperature in the upper atmosphere," Space Research, 3, 282, 1963.

Hanson, W.B., and Robert Cohen, "Photoelectron heating efficiency in the ionosphere," J. Geophys. Res., 73, 831, 1968.

Hoegy, W.R., Jean-Pierre Fournier, and E.G. Fontheim, "Photoelectron energy distribution in the F region," J. Geophys. Res., 70, 5464, 1965.

Maier, E.J., and B.C. Narasinga Rao, "Rocket measurements of conjugate photoelectrons during total solar eclipse of March 7, 1970 over Wallops Island," paper A7.3, COSPAR, Fourteenth Plenary Meeting, Seattle, Washington, June 1971.

Nagy, A.F. and P.M. Banks, "Photoelectrons fluxes in the ionosphere," J. Geophys. Res., 75, 6260, 1970.

Nisbet, J.S., "Photoelectron escape from the ionosphere," J. Atmos. Terr. Phys., 30, 1257, 1968.

Rishbeth, H., "Solar eclipses and ionospheric theory," Space Sci. Rev., 8, 543, 1968.

Smith L.G., "Rocket observations of solar UV radiation during the eclipse of 7 March 1970," paper A4.4, COSPAR, Fourteenth Plenary Meeting, Seattle Washington, June 1971.